BMC Medical Genomics

RESEARCH

Open Access

Integrated bioinformatics analysis and experimental validation reveal the relationship between ALOX5AP and the prognosis and immune microenvironment in glioma

Ping Song[1], Hui Deng[1], Yushu Liu[1] and Mengxian Zhang[1*]

Abstract

Background Treatment of gliomas, the most prevalent primary malignant neoplasm of the central nervous system, is challenging. Arachidonate 5-lipoxygenase activating protein (ALOX5AP) is crucial for converting arachidonic acid into leukotrienes and is associated with poor prognosis in multiple cancers. Nevertheless, its relationship with the prognosis and the immune microenvironment of gliomas remains incompletely understood.

Methods The differential expression of ALOX5AP was evaluated based on public Databases. Kaplan–Meier, multivariate Cox proportional hazards regression analysis, time-dependent receiver operating characteristic, and nomogram were used to estimate the prognostic value of ALOX5AP. The relationship between ALOX5AP and immune infiltration was calculated using ESTIMATE and CIBERSORT algorithms. Relationships between ALOX5AP and human leukocyte antigen molecules, immune checkpoints, tumor mutation burden, TIDE score, and immunophenoscore were calculated to evaluate glioma immunotherapy response. Single gene GSEA and co-expression network-based GO and KEGG enrichment analysis were performed to explore the potential function of ALOX5AP. ALOX5AP expression was verified using multiplex immunofluorescence staining and its prognostic effects were confirmed using a glioma tissue microarray.

Result ALOX5AP was highly expressed in gliomas, and the expression level was related to World Health Organization (WHO) grade, age, sex, IDH mutation status, 1p19q co-deletion status, MGMTp methylation status, and poor prognosis. Single-cell RNA sequencing showed that *ALOX5AP* was expressed in macrophages, monocytes, and T cells but not in tumor cells. *ALOX5AP* expression positively correlated with M2 macrophage infiltration and poor immunotherapy response. Immunofluorescence staining demonstrated that ALOX5AP was upregulated in WHO higher-grade gliomas, localizing to M2 macrophages. Glioma tissue microarray confirmed the adverse effect of ALOX5AP in the prognosis of glioma.

*Correspondence:
Mengxian Zhang
zhangmx73@163.com

Full list of author information is available at the end of the article

Conclusion ALOX5AP is highly expressed in M2 macrophages and may act as a potential biomarker for predicting prognosis and immunotherapy response in patients with glioma.

Keywords Glioma, ALOX5AP, Multiplex immunofluorescence, Tumor-associated macrophage, Prognosis

Introduction

Gliomas are the most prevalent primary brain tumors, accounting for 80–85% of adult malignant brain tumors [1]. Gliomas can be categorized into four grades according to biological characteristics, with World Health Organization (WHO) grade 2 and 3 considered lower-grade gliomas (LGG). Alternatively, WHO grade 4 glioblastomas (GBM) have the worst prognosis, with only 6.8% five-year overall survival (OS) rate [2, 3]. Tumor-associated macrophages (TAMs) account for approximately 50% of the total tumor mass and 30–50% of the total cell count in the GBM tumor microenvironment (TME) [4, 5]. TAMs in GBM consist of bone marrow-derived macrophages (85%) and resident microglia (15%) and exhibit spatially and temporally specific [6]. TAMs differentiate into antitumor M1 (classical) or pro-tumor M2 (alternative pathway) types [7]. Preclinical studies have shown that macrophages are important in glioblastoma immune evasion. Immunosuppressed tumor-associated macrophages interact with and exhausted T cells, decreasing their antitumor response [8]. The clinical value of immune checkpoint blockade therapy has been confirmed in a wide range of tumors, but not in gliomas. In particular, anti-PD-1 treatment alters the TAM phenotype, preventing optimal T-cell activation [9]. It is therefore necessary to identify new macrophage targets that can affect the glioma TME in order to improve the efficacy of therapeutic interventions.

Arachidonic acid (AA), a polyunsaturated fatty acid released from membrane phospholipids, serves as a precursor for eicosanoid biosynthesis [10]. AA produces prostaglandins and thromboxane through the cyclooxygenase pathway and leukotrienes and lipoxins through the lipoxygenase (LOX) pathway [10]. The LOX pathway is regulated by arachidonate 5-lipoxygenase-activating protein (ALOX5AP, also termed FLAP). In a complex with nuclear ALOX5, ALOX5AP efficiently generates 5-hydroperoxy eicosatetraenoic acid (5-HETE) from AA. 5-HETE is then converted to various leukotrienes [11]. As leukotriene signaling mediates inflammation and atherosclerosis, ALOX5AP is associated with cardiovascular, cerebrovascular, and inflammatory diseases [12, 13]. ALOX5AP has been identified as a prognostic marker of e.g. osteosarcoma [14], ovarian cancer [15], lower-grade gliomas [16]. However, the correlation between ALOX5AP levels and gliomas has not been comprehensively evaluated.

Therefore, the main study objectives were to investigate ALOX5AP expression (1) at both the bulk and single-cell level and (2) among various subgroups based on glioma clinical characteristics; and its (3) correlation with the TME; (4) relationships with immunotherapy response and drug sensitivity; (5) association with potentially significant pathways in gliomas; and (6) relationship with the prognosis of patients with glioma.

Methods

Data

Bulk RNA-Seq and simple nucleotide variation data of glioma samples were obtained from The Cancer Genome Atlas (TCGA) [17] and Chinese Glioma Genome Atlas (CGGA) [18] databases; samples with complete survival information and clinical significance were included. Two newly diagnosed GBM (ndGBM_02 and ndGBM_03) and two LGG (LGG_03 and LGG_04) samples were selected from the glioma single-cell RNA-Seq dataset (GSE182109; Gene Expression Omnibus (GEO) database) [19].

ALOX5AP expression analysis

ALOX5AP expression in normal and glioma samples was analyzed using Tumor Immune Estimation Resource (TIMER)2.0 [20] and Gene Expression Profiling Interaction Analysis (GEPIA) [21] databases. Comparison of *ALOX5AP* expression levels was conducted among various clinical subgroups, encompassing grade, age, sex, and isocitrate dehydrogenase (IDH) mutation status, 1p19q codeletion status, O^6-methylguanine-DNA methyltransferase promoter (MGMTp) status, radio status, and temozolomide (TMZ) status.

Prognostic analysis

Based on the optimal cutoff value of *ALOX5AP* expression calculated using "survminer" in R, the TCGA and CGGA cohorts were divided into high and low expression groups. Kaplan–Meier analysis and the log-rank test were used to assess the between-group difference in OS time. Multivariate COX proportional hazards regression analysis was used to demonstrate the independent prognostic effect of *ALOX5AP*. The efficacy of *ALOX5AP* for evaluating 1-, 3-, and 5-year survival was examined using time-dependent receiver operating characteristic (time-ROC) curve analysis. ALOX5AP, WHO grade, sex, age, IDH mutation status, 1p19q codeletion status, and MGMTp methylation status were used to construct a nomogram, and then the calibration curve and the concordance index were calculated to assess predictive performance of the nomogram.

Single-cell RNA-Seq

Single cell RNA-Seq data analysis and quality control of the newly diagnosed GBM and LGG samples were performed using the 'Seurat' R package. The cells and genes were excluded according to the following criteria: (1) genes expressed in <3 cells; (2) cells with a total mapped unique molecular identifier<1000; (3) cells with <500 detected genes; and (4) cells with >20% unique mitochondrial molecular identifiers, yielding a total of 55,327 cells. Subsequently, data dimensionality was reduced using principal component analysis. The 'Seurat' R 'FindClusters' function was used for cell clustering analysis, and 'infercnv' for tumor cell detection. Marker genes for each cluster were identified using 'FindAllMarkers' with filtering conditions: $\log_2$|fold change| ≥0.5, pct.1−pct.2≥0.25, and $P<0.05$. The cell clusters were annotated using ScType software and visualized using Uniform Manifold Approximation and Projection [22, 23]. To validate *ALOX5AP* expression in gliomas across cell types, we selected datasets GSE70630, GSE84465, GSE131928_10X, and GSE89567 from The Tumor Immune Single Cell Hub 2 (TISCH2), a tumor microenvironment-associated single-cell RNA database that provides single-cell-level cell type annotations [24].

Relationship between ALOX5AP and immune infiltration

The immune-related features of ALOX5AP were examined using the ESTIMATE and CIBERSORT algorithms. The ESTIMATE algorithm comprises four scoring systems: stromal (which positively correlates with stroma presence), immune (which positively correlates with immune cell infiltration extent), estimate (which negatively correlates with tumor purity), and tumor purity (i.e., the proportion of tumor cells to all cells in the sample) [25]. The CIBERSORT algorithm was employed to calculate the fractions of 22 immune-infiltrating cells in glioma tissue [26]. To investigate the correlation between *ALOX5AP* expression and different TME components, including immunosuppressive factors, chemokines, and chemokine receptors, the TISIDB website [27] was utilized.

Immunotherapy response and drug sensitivity prediction

The R packages 'ggpubr' and 'corrplot' were used to analyze the differential expression of human leucocyte antigen (HLA) and immune checkpoint and their correlation with ALOX5AP. The 'Maftool' R package was used to calculate the tumor mutation burden (TMB) of each sample in TCGA samples. The Cancer Immunome Atlas (TCIA) was used to assess the response to CTLA-4 or PD-1 blockade of each TCGA-GBM sample through the immunophenoscore (IPS) [28]. The Tumor Immune Dysfunction and Exclusion (TIDE) website [29] was used to calculate the TIDE score for each sample. Cancer cell sensitivity and drug response molecular markers data resource were download from Genomics of Drug Sensitivity in Cancer (GDSC) database [30]. Drug sensitivity analysis was performed using the 'OncoPredict' R package to calculate half maximal inhibitory concentration for 13 common chemotherapy drugs.

Enrichment analysis and protein–protein interaction (PPI) network

Gene Set Enrichment Analysis (GSEA) was utilized to conduct enrichment analyses of ALOX5AP-associated functions and pathways [31]. The R packages 'Limma', 'Org.Hs.eg.db', 'ClusterProfiler', and 'Enrichplot' were used to conduct GSEA and mapping. The criteria for selecting enrichment pathways included a false discovery rate<0.25, $P<0.05$, and normalized enrichment score≥1. The 72 key proteins with correlation coefficients>0.4 with ALOX5AP were screened using the STRING database [32] and visualized using Cytoscape software [33]. The 72 genes were analyzed using 'ClusterProfiler', 'Org.Hs.eg.db', and 'Stringi' R packages for Gene Ontology (GO) and Kyoto Encyclopedia of Genomes (KEGG) Enrichment Analysis.

Tissue microarray and multiplex immunofluorescence

A tissue microarray with clinical information was obtained from Outdo Biotech Company (Table S1). Immunofluorescence was performed using the Opal 7-Color Manual IHC Kit (NEL801001KT, PerkinElmer) and VECTASHIELD® HardSet Antifade Mounting Medium (H-1400, Vector Labs). Primary antibodies included anti-ALOX5AP (rabbit, 1:500, HPA026592, Atlas), anti-CD163 (rabbit, 1:500, 93498, Cell Signaling Technology), and anti-CD68 (rabbit, 1:1, PA014, Baidao Medical Technology). Immunofluorescence staining method has been previously reported [34].

Fluorescence signal quantification

Panoramic multispectral slide scanning was performed using the Tissue-FAXS Spectra system (Tissue Gnostics). Subsequently, the data was imported into StrataQuest analysis software, where spectral splitting was conducted with the assistance of a spectral library, thereby enabling the acquisition of individual fluorescence signals for each channel. Active nuclei were identified using the DAPI channel. To locate the protein fluorescence staining signal, a core was formed using an efficient nucleus, and the distance radius was determined based on the staining intensity of each protein channel. A threshold was established based on antibody fluorescence intensity and area considering the staining in each channel, and used to separate the population of positive cells and determine their number.

Statistical analysis

All statistical analyses were calculated using R software (4.3.2) or GraphPad Prism 10. The Kruskal–Wallis test was utilized to analyze all multiple-group comparisons. For normally distributed data, the Student's t-test was used for between-group comparisons; otherwise, the Mann–Whitney test was used. Spearman's correlation analysis was used for all correlation analyses. $P<0.05$ was considered statistically significant.

Results

ALOX5AP is highly expressed in glioma and correlates with clinical features

ALOX5AP expression in glioma was investigated using the TIMER2.0 database, comprising 153 GBM and five normal samples. The GEPIA database, including 163 GBM, 518 LGG, and 207 normal samples, was used to evaluate *ALOX5AP* differential expression between glioma and normal tissue. These results indicated that *ALOX5AP* was highly expressed in gliomas (Fig. 1A, B).

To examine the correlation with glioma clinical characteristics, we analyzed *ALOX5AP* expression in the CGGA cohort. *ALOX5AP* expression was higher in patients with WHO grade 4 GBM than in those with grade 2–3 glioma ($P<2.2e-16$) (Fig. 1C), in patients aged ≥ 40 years ($P=5.3e-04$) (Fig. 1D), in male ($P=9.8e-06$) (Fig. 1E), and in the IDH wild-type ($P<2.2e-16$) (Fig. 1F), 1p19q non-codeletion ($P=2.2e-16$) (Fig. 1G), and MGMTp unmethylated groups ($P<1.2e-03$) (Fig. 1H). However, *ALOX5AP* expression was not correlated with TMZ chemotherapy ($P=7.1e-01$) or radiotherapy ($P=3.2e-01$) (Fig. 1I, J).

ALOX5AP predicts worse survival in glioma

In the CGGA database, high *ALOX5AP* expression correlated with shorter OS in different subgroups, based on age, sex, 1p19q codeletion status, IDH mutation status, MGMTp methylation status, and grade (all $P<0.05$) (Fig. 2A–F). For TCGA, higher *ALOX5AP* expression correlated with decreased OS in both TCGA-LGG ($P<0.001$) (Fig. S1A) and TCGA-GBM samples ($P=0.018$) (Fig. S1B). Multivariate COX proportional hazards regression analysis based on the TCGA cohort showed that ALOX5AP was an independent prognostic factor for glioma (Table. S2).

Based on the area under the curve (AUC) of time-ROC, ALOX5AP expression accurately predicted glioma OS at 1 (CGGA: 0.612; TCGA: 0.796), 3 (CGGA: 0.663; TCGA: 0.772), 5 (CGGA:0.687; TCGA: 0.744), and 10 years (CGGA: 0.678; TCGA: 0.804) (Fig. 3A, B). A nomogram was created by combining ALOX5AP expression data with clinical prognostic factors, including WHO grade, age, sex, and IDH mutation, 1p19q codeletion, and MGMTp methylation status (Fig. 3C). Nomogram performance was evaluated by calibration, resulting in a concordance index of 0.739 for OS (Fig. 3D). Both ALOX5AP and nomogram findings demonstrated reliable predictive efficacy for OS, as evidenced by the elevated AUC and concordance index.

ALOX5AP is mainly expressed in TAMs but not in tumor cells

To assess *ALOX5AP* expression at the single-cell level, we conducted single-cell RNA-Seq analysis on two newly diagnosed GBM and two LGG samples based on GSE182109. Cells were divided into 25 clusters with 11 identified cell types: astrocytes, endothelial cells, macrophages, microglia, monocytes, neural stem cells, neurons, oligodendrocytes, pericytes, Schwann precursors, and T cells (Fig. 4A and Table S3). *ALOX5AP* was significantly expressed in the macrophages, microglia, monocytes, and T cells of both LGG and GBM (Fig. 4B). According to the GSE70630, GSE84465, GSE131928_10X, and GSE89567 datasets, the TISCH2 database also revealed significant *ALOX5AP* expression in GBM macrophages, monocytes, and T cells (Fig. 4C).

ALOX5AP association with immune infiltration in glioma

In view of the fact that ALOX5AP is mainly expressed in immune cells, especially macrophages, rather than tumor cells in gliomas. We calculated the correlation between ALOX5AP and the immune, estimate, tumor purity, and stroma scores in the CCGA cohort using the ESTIMATE algorithm. High *ALOX5AP* expression was associated with higher immune, estimate, and stromal scores, albeit lower tumor purity (all $P<0.001$) (Fig. 5A–D), suggestive of high levels of immune infiltration.

The correlation between ALOX5AP and 22 diverse types of immune cells in glioma was analyzed using the CIBERSORT algorithm based on the CGGA cohort. High *ALOX5AP* expression was associated with greater M2 macrophage ($P<0.001$) and neutrophil ($P<0.01$) proportions, whereas low *ALOX5AP* expression related to larger naive CD4+T cell ($P<0.01$), helper follicular cell ($P<0.05$), activated mast cell ($P<0.01$), and resting dendritic cell fractions ($P<0.05$) (Fig. 5E).

The relationship between ALOX5AP and immunosuppressive factors, chemokines, and chemokine receptors in GBM was analyzed using the TISIDB database. The top three immunosuppressive factors (*CSF1R*, *HAVCR2*, and *IL10*), chemokine (*CCL20*, *CCL16*, and *CXCL2*), and chemokine receptor genes (*CCR1*, *CCR2*, and *CCR5*) correlating with *ALOX5AP* and the correlation coefficients between *ALOX5AP* and the immune component genes in the TISIDB database are shown in Fig. 5G–I and Table S4.

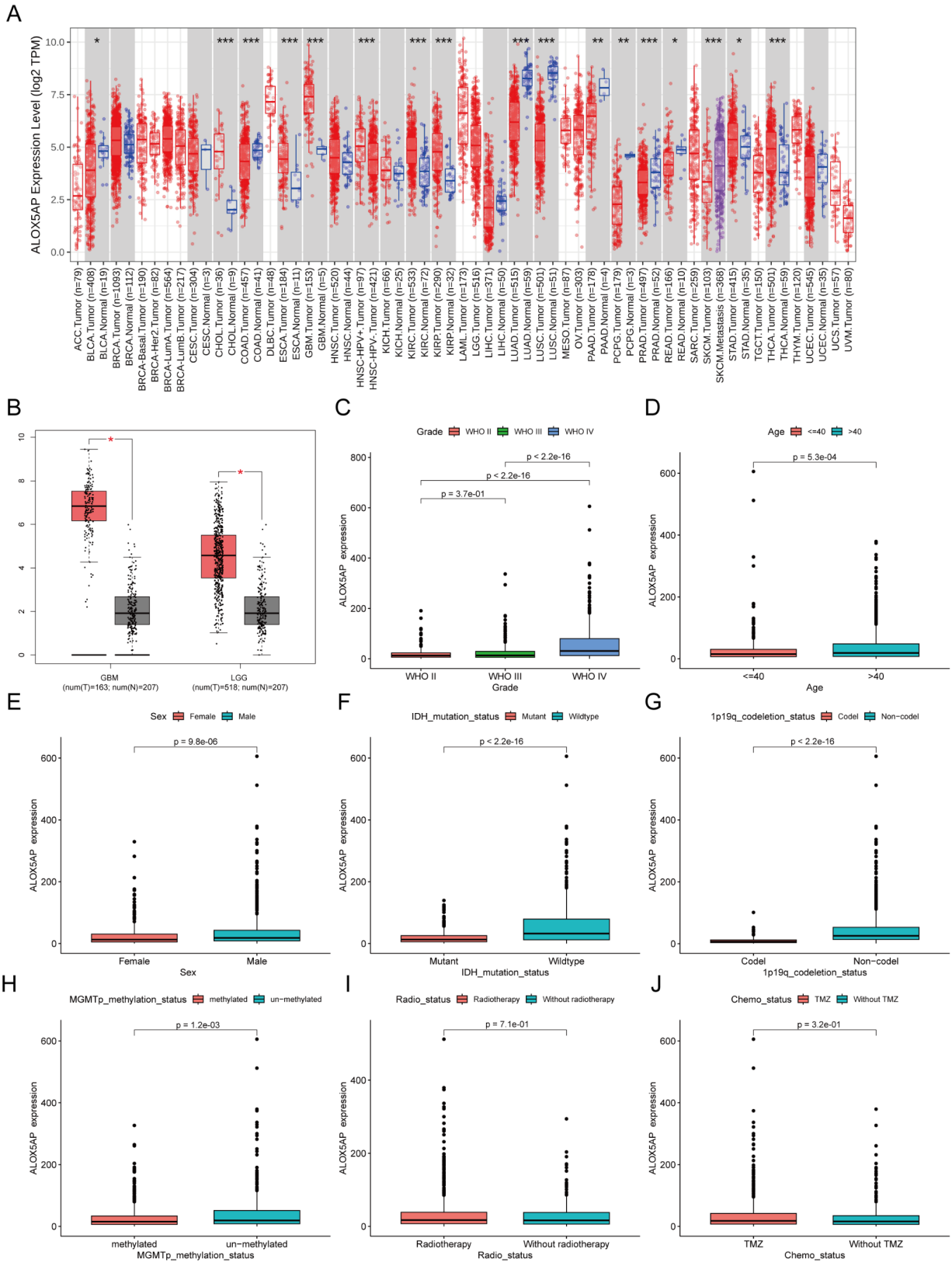

Fig. 1 Expression of ALOX5AP. **A**, **B** Expression of ALOX5AP in the normal and tumor samples in TIMER2.0 and GEPIA online databases. Expression of ALOX5AP in gliomas of different **C** grade, **D** age, **E** sex, **F** IDH mutation status, **G** 1p19q codeletion status, **H** MGMTp methylation status, **I** radio status, **J** TMZ status based on CGGA database. **P* < 0.05, ***P* < 0.01, ****P* < 0.001

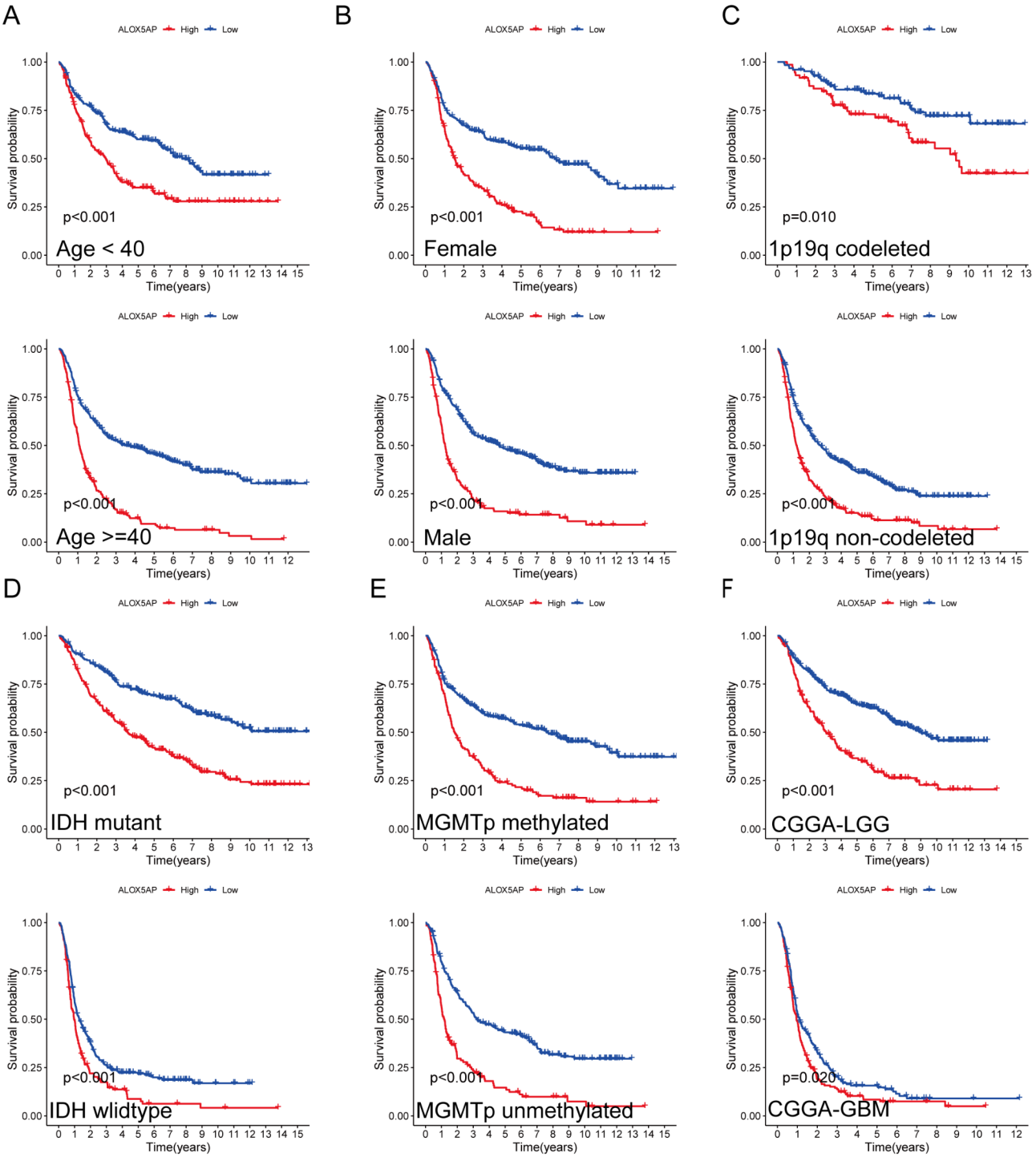

Fig. 2 Prognostic analysis of ALOX5AP in glioma patients based on CGGA samples. Kaplan-Meier survival curve of CGGA samples in different subgroups, including **A** age, **B** sex, **C** 1p19q codeletion status, **D** IDH mutation status, **E** MGMTp methylation status and **F** WHO grades

Correlation of ALOX5AP expression with immunotherapies and chemotherapeutics drugs sensitivity in glioma

It is believed that TMB is associated with response to immunotherapy in a wide range of tumors [35]. Mutations are processed into neoantigens and are presented to T cells by HLA molecules [36]. TMB, HLA molecules, and immune checkpoints can serve as a part of predicting the outcome of immunotherapy [36]. We calculated the correlation between ALOX5AP and several biomarkers, including HLA (HLA-A, HLA-B, HLA-C, HLA-E,

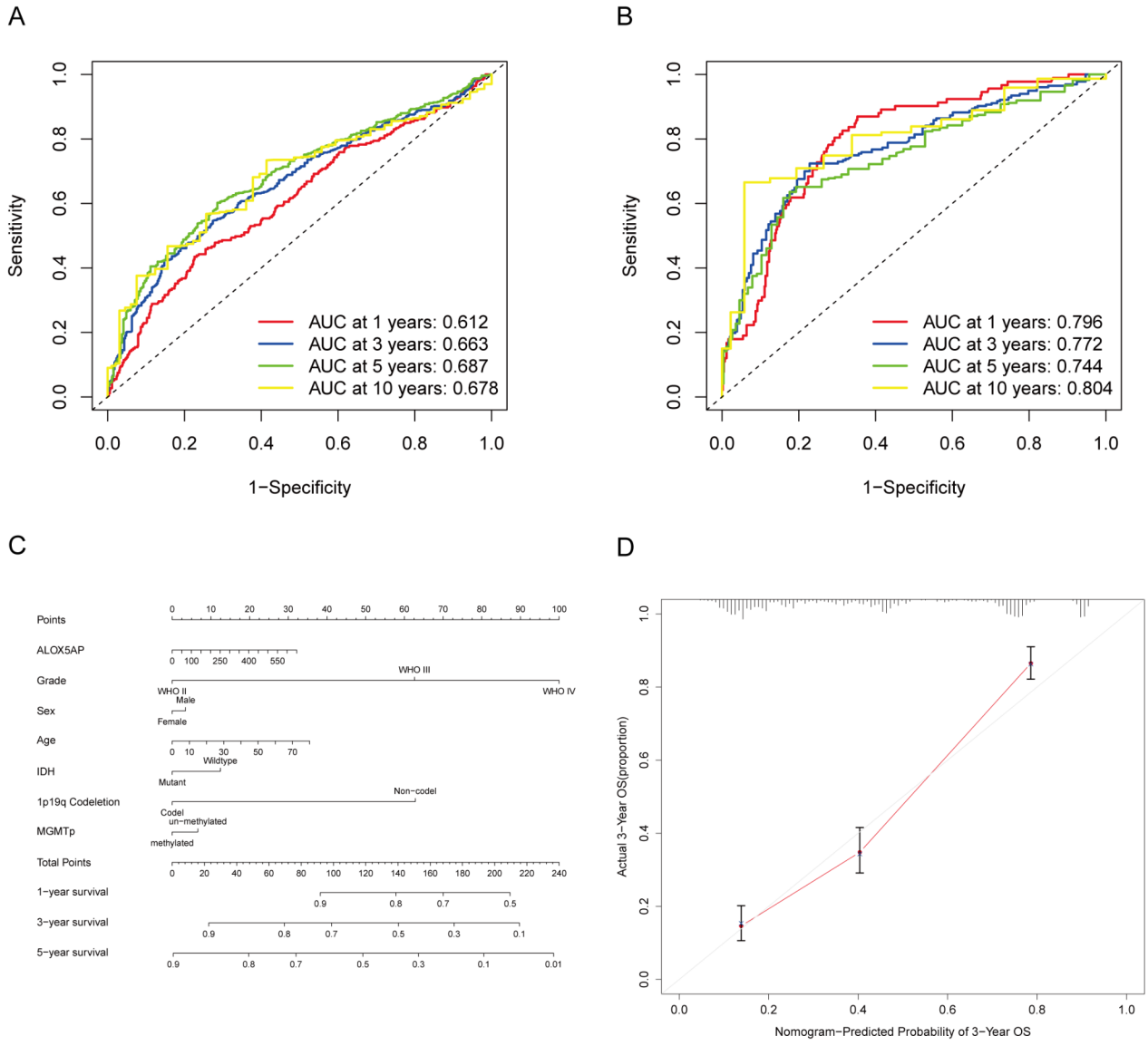

Fig. 3 Prognostic prediction of ALOX5AP in glioma patients. **A–B** time-ROC curve predictive accuracy of ALOX5AP in CGGA cohort and TCGA cohort for OS at 1-, 3-, 5-, and 10-years. **C** The nomogram from CGGA cohort. **D** Prediction of the calibration curve from CGGA cohort

HLA-F, HLA-DMA, HLA-DMB, HLA-DOA, HLA-DOB, HLA-DPA1, HLA-DPB2, HLA-DQA1, HLA-DQB1, HLA-DRA, HLA-DRB1, and HLADRB5), and immune checkpoints (IDO1, CTLA4, LAG3, CD47, CD160, CD244, BTLA, ICOS, PDCD1, HAVCR2, CD276, TNFSF4, CD80, ARHGEF5, and VTCN1). *ALOX5AP* was significantly positively associated with most of the biomarkers which also showed upregulated in high ALOX5AP group in both CGGA (Fig. 6A–B) and TCGA samples (Fig. S2A–B).

Afterward, we explored TMB in the *ALOX5AP* high and low expression groups. The result showed that the *ALOX5AP* high expression group had a higher TMB (P=2.9e−16) (Fig. 7A). We used the TCIA database to evaluate the immunotherapy response of TCGA-GBM samples through IPS, and a higher IPS signifies a better response to immunotherapy. The results revealed that the IPS of CTLA-4 negative PD-1 negative and CTLA-4 negative PD-1 positive groups in the low *ALOX5AP* expression group were significantly higher than that in the high ALOX5AP expression group (Fig. 7B, C), which strongly predicted that GBM patients with lower *ALOX5AP* expression would benefit immunotherapy. In comparison, the IPS of CTLA-4 positive PD-1 negative and CTLA-4 positive PD-1 positive groups did not differ significantly between *ALOX5PA* high and low groups (Fig. 7D, E). Based on TCGA and CGGA samples, the high *ALOX5AP* expression group had higher TIDE scores

Fig. 4 Expression of ALOX5AP in single cell level. **A** Clustering and annotation of glioma in GSE180192 yielded 25 clusters and 11 cell types. **B** Expression of ALOX5AP in 25 clusters and 11 cell types. **C** Expression of ALOX5AP in various cell types in GSE70630, GSE84465, GSE131928_10X, and GSE89567 based on TISCH2 online database

(TCGA: P=3.8e−07; CGGA: P=1.5e−09) (Fig. 7F, G), suggesting that ALOX5AP is associated with immune evasion. Moreover, the expression of *ALOX5AP* was positively correlated with TIDE score (TCGA: R=0.23, P=1.3e−09; CGGA: R=0.26, P=2.2e−16) (Fig. 7H, I).

Given that chemotherapy is one of the critical means of glioma treatment in the clinic, we next calculated the sensitivity of glioma to 13 drugs, including camptothecin, vincristine, cisplatin, cytarabine, docetaxel, 5-fluorouracil, paclitaxel, irinotecan, oxaliplatin, gemcitabine, temozolomide, epirubicin, cyclophosphamide, and carmustine. The *ALOX5AP* high expression group was less sensitive to vincristine, cytarabine, temozolomide, and carmustine, and more sensitive to 5-fluorouracil and irinotecan. Glioma sensitivity to docetaxel and gemcitabine was not associated with *ALOX5AP* (Fig. 7J, K).

The signaling pathway associated with ALOX5AP

To investigate the biological function of ALOX5AP in glioma, GSEA was conducted based on the TCGA database. In GBM, the top five signaling pathways of GO terms are chemokine receptor binding, immunoglobulin complex

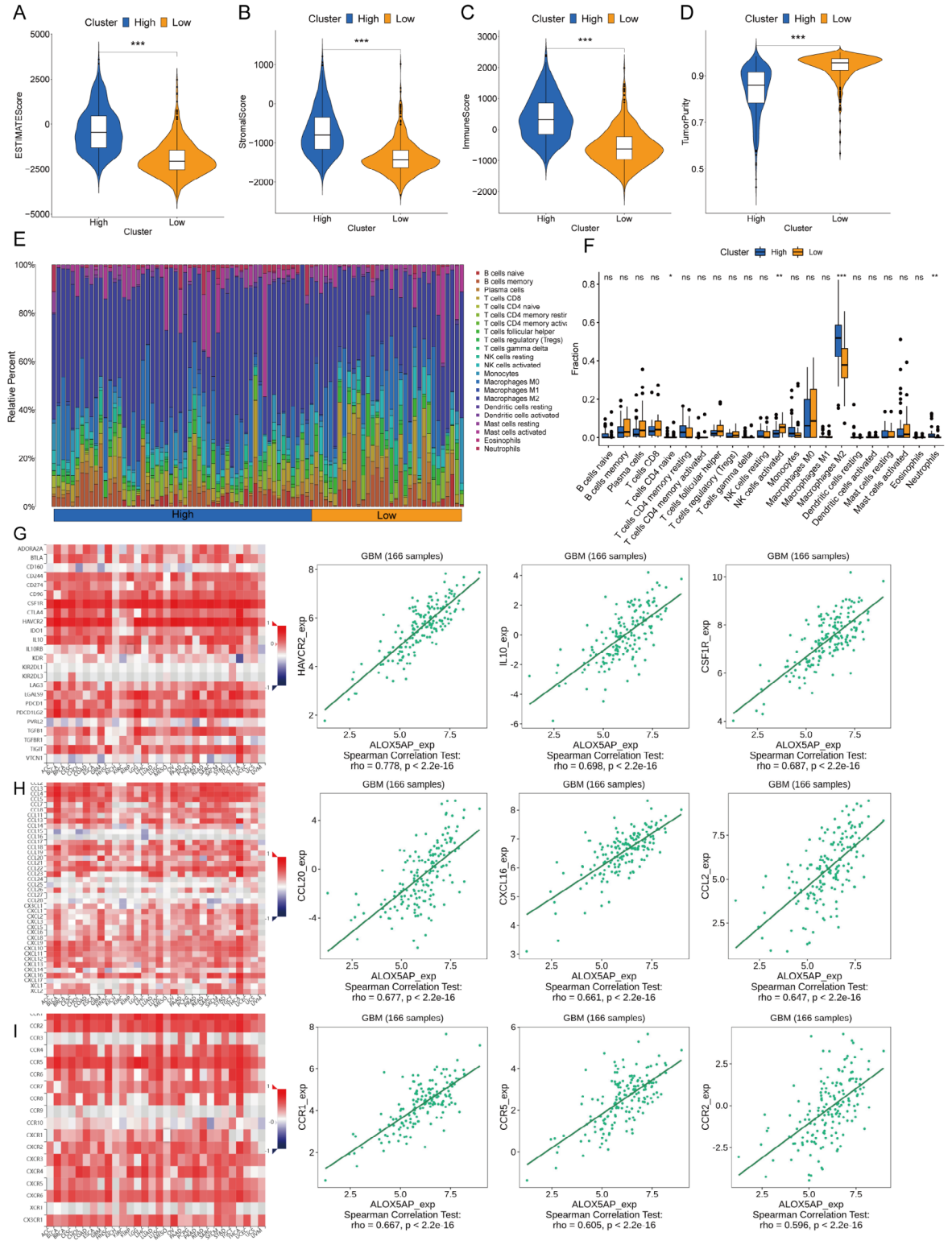

Fig. 5 Relationship between ALOX5AP and immune infiltration in glioma. **A–D** Relationship between ALOX5AP and estimate score, immune score, tumor purity, and stroma score analyzed by ESTIMATE algorithm based on CGGA cohort. **E**, **F** Relationship between ALOX5AP and 22 types of immune cells analyzed by CIBERSORT algorithm based on CGGA cohort. **G–I** Relationship between ALOX5AP and immunosuppressive factors, chemokines, and chemokine receptors in the TISIDB database and scatterplots of the three highest correlation coefficients are presented. *$P < 0.05$, **$P < 0.01$, ***$P < 0.001$, ns = no significance

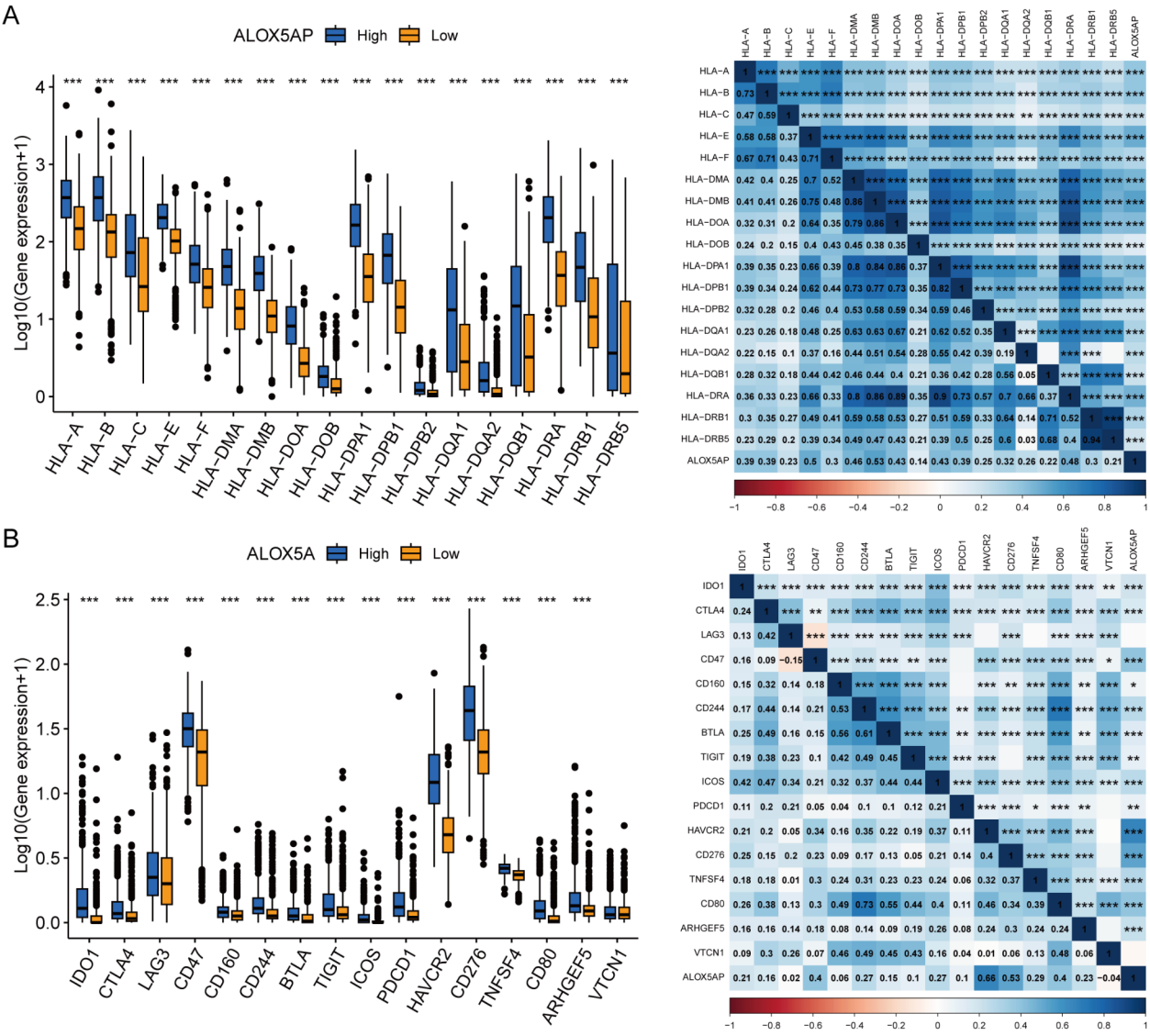

Fig. 6 Analysis of HLA and immune checkpoints based on CGGA cohort. **A** Differential expression of HLA in ALOX5AP high and low groups and the correlation between ALOX5AP and HLA. **B** Differential expression of immune checkpoints in ALOX5AP high and low groups and the correlation of ALOX5AP and immune checkpoints. *$P < 0.05$, **$P < 0.01$,***$P < 0.001$.

circulating, immunoglobulin receptor binding, phagocytosis recognition, and response to chemokine (Fig. 8A); the top five signaling pathways of KEGG terms are graft versus host disease, hematopoietic cell lineage, intestinal immune network for IGA production, leishmania infection, and NOD-like receptor signaling pathway (Fig. 8B). In LGG, the top five signaling pathway of GO terms are B cell-mediated immunity, human immune response mediated circulating immunoglobulin, immunoglobulin complex circulating, and immunoglobulin receptor binding (Fig. 8C); the top five signaling pathway of KEGG terms are allograft rejection, cytokine-cytokine receptor, graft versus host disease, hematopoietic cell lineage, leishmania infection (Fig. 8D).

The interacting proteins of ALOX5AP were screened using the STRING database; the 71 strongest interacting proteins were visualized using Cytoscape (Fig. 8E). GO and KEGG enrichment analyses were performed for the 72 respective protein-encoding genes, including *ALOX5AP*. The top five BP, CC, and MF terms according to *P* values are shown in Fig. 8F. The top 20 KEGG-enriched pathways were eicosanoid metabolism, arachidonic acid metabolism, fatty acid biosynthesis, myeloid leukocyte activation, neuroinflammatory response, glial cell activation, microglia activation, and leukocyte activation involved in inflammatory response, etc. (Fig. 8G). These results suggest that ALOX5AP plays a fundamental role in TME.

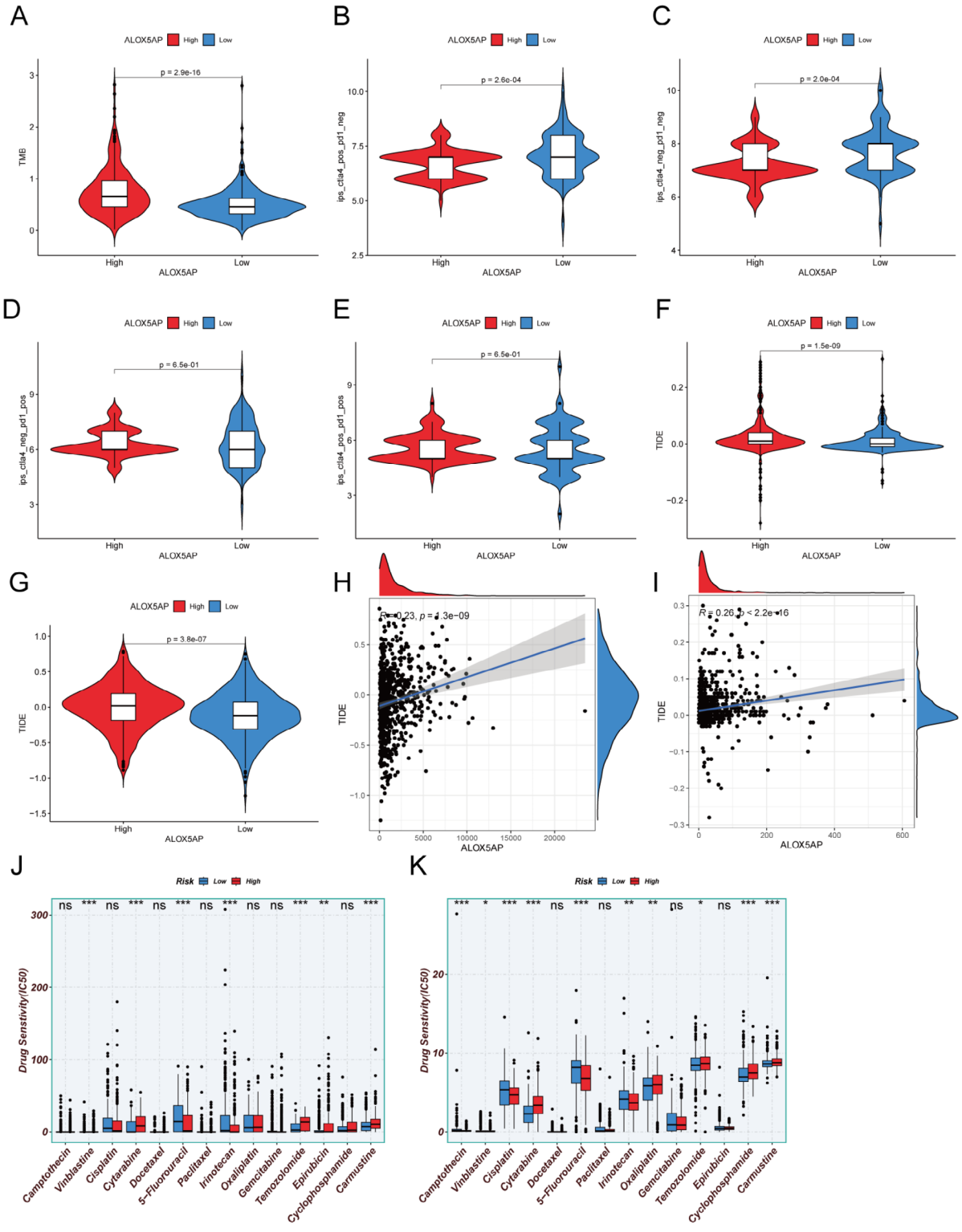

Fig. 7 The relationship of ALOX5AP to immunotherapy response and drug sensitivity. **A** The significantly different distributions of the TMB in ALOX5AP high and low groups based on TCGA samples. **B–E** Comparison of IPS of patients with different risk groups. **F**, **G** The significantly different distributions of the TIDE score in ALOX5AP high and low groups based on TCGA and CGGA samples. **H**, **I** Correlation between ALOX5AP expression and TIDE score based on TCGA and CGGA samples. **J**, **K** Comparison of the sensitivity of patients with different risk groups to common chemotherapeutics based on TCGA and CGGA samples. (Half maximal inhibitory concentration: IC50) $^{*}P < 0.05$, $^{**}P < 0.01$, $^{***}P < 0.001$, ns = no significance

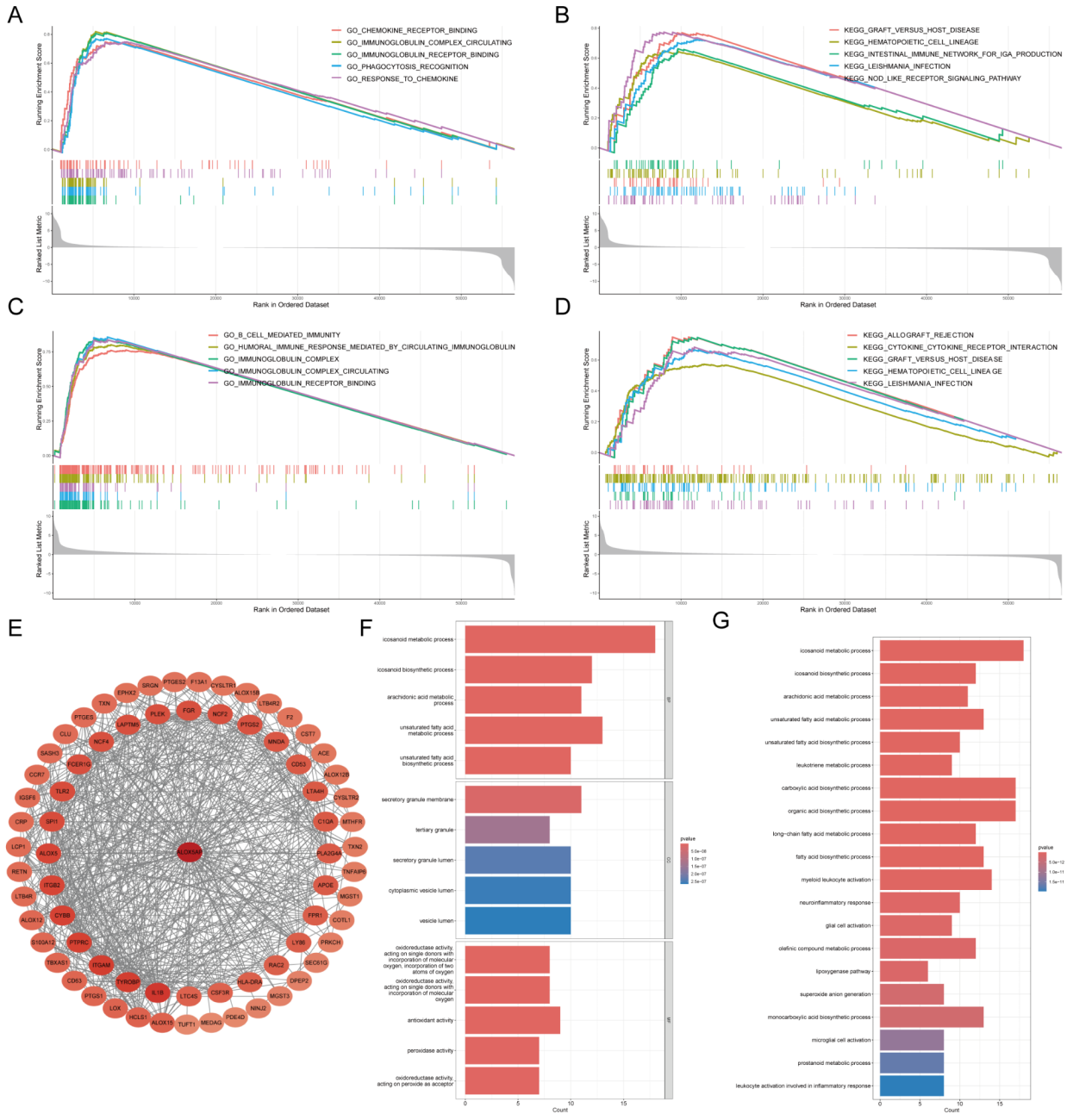

Fig. 8 Functional enrichment analysis of ALOX5AP. **A** The top 5 enriched pathways of GBM in GSEA based on GO terms. **B** The top 5 enriched pathways of GBM in GSEA based on KEGG terms. **C** The top 5 enriched pathways of LGG in GSEA based on GO terms. **D** The top 5 enriched pathways of LGG in GSEA based on KEGG terms. **E** Top 71 proteins with the highest correlation coefficient with ALOX5AP from STRING database; **F** GO enrichment analysis of ALOX5AP and ALOX5AP related genes; **G** KEGG enrichment analysis of ALOX5AP and ALOX5AP related genes

Validation of ALOX5AP expression in glioma tissue

Our bioinformatics analyses demonstrated that ALOX5AP was expressed in macrophages and positively correlated with the M2 macrophage fraction. To confirm the bioinformatics findings, we employed multiplex immunofluorescence staining of ALOX5AP, CD163 (M2 macrophage marker), and CD68 (M0 macrophage marker) in a glioma tissue microarray (Fig. 9A). ALOX5AP+and CD163+cell percentages were increased in WHO grade 4 compared to grade 2–3 gliomas (all $P<0.05$) (Fig. 9B, C), whereas CD68+cell percentage showed no grade-specific difference (Fig. 9D). Moreover, ALOX5AP co-localized with CD68 and CD163 in gliomas (Fig. 10A). The

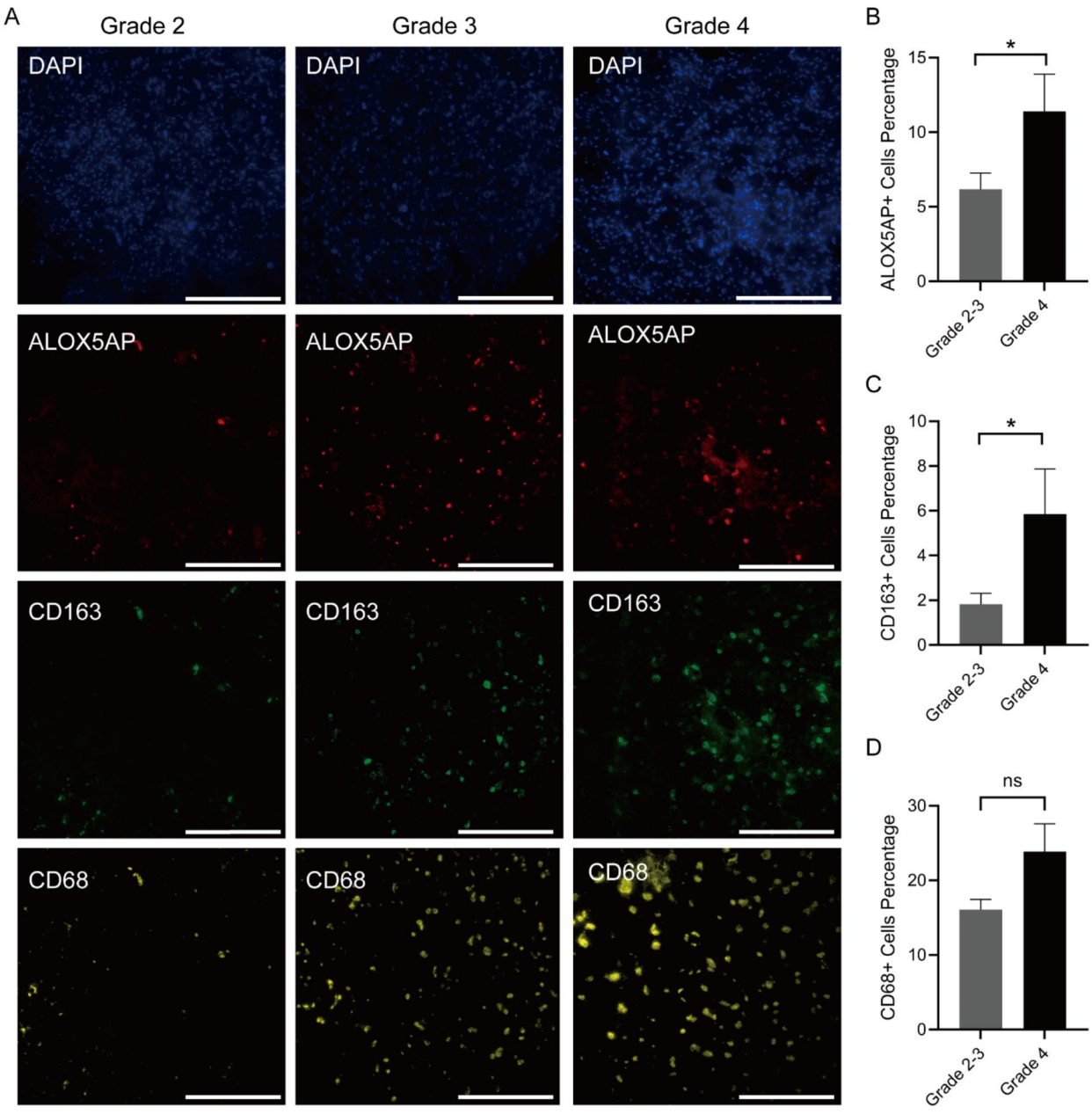

Fig. 9 Multiplex immunofluorescence staining of ALOX5AP (red), CD163 (green) and CD68 (yellow) protein in glioma tissue microarray with different grades. **A** Representative immunofluorescence image of ALOX5AP, CD163, and CD68 expression in WHO grade 2, grade 3, and grade 4 glioma. (The scale bar is 200 μm). **B–D** Quantitative analysis of ALOX5AP+, CD163+, and CD68 + cells percentage in WHO grade 2–3 and grade 4 glioma samples. *$P < 0.05$, ns = no significance

group with high ALOX5AP + cell percentage had higher CD68 + and CD163 + cell percentages than those in the low-percentage ALOX5AP + cells in both WHO grade 2–3 (all $P < 0.05$) and grade 4 gliomas (all $P < 0.05$) (Fig. 10B–E). Spearman's correlation analysis showed that ALOX5AP + cell percentage positively correlated with CD163 + cell percentage ($R = 0.4$, $P = 1.8e{-}05$) and CD68 + cell percentage ($R = 0.43$, $P = 3.6e{-}06$) in the glioma tissue microarray (Fig. 10F, G).

To verify the prognostic value of ALOX5AP in glioma, we performed Kaplan–Meier analysis and time-ROC curve based on the glioma tissue microarray. High ALOX5AP + cell percentage correlated with worse OS in 109 glioma samples ($P = 0.023$) (Fig. 10H). In the glioma tissue microarray, ALOX5AP + cell percentage similarly

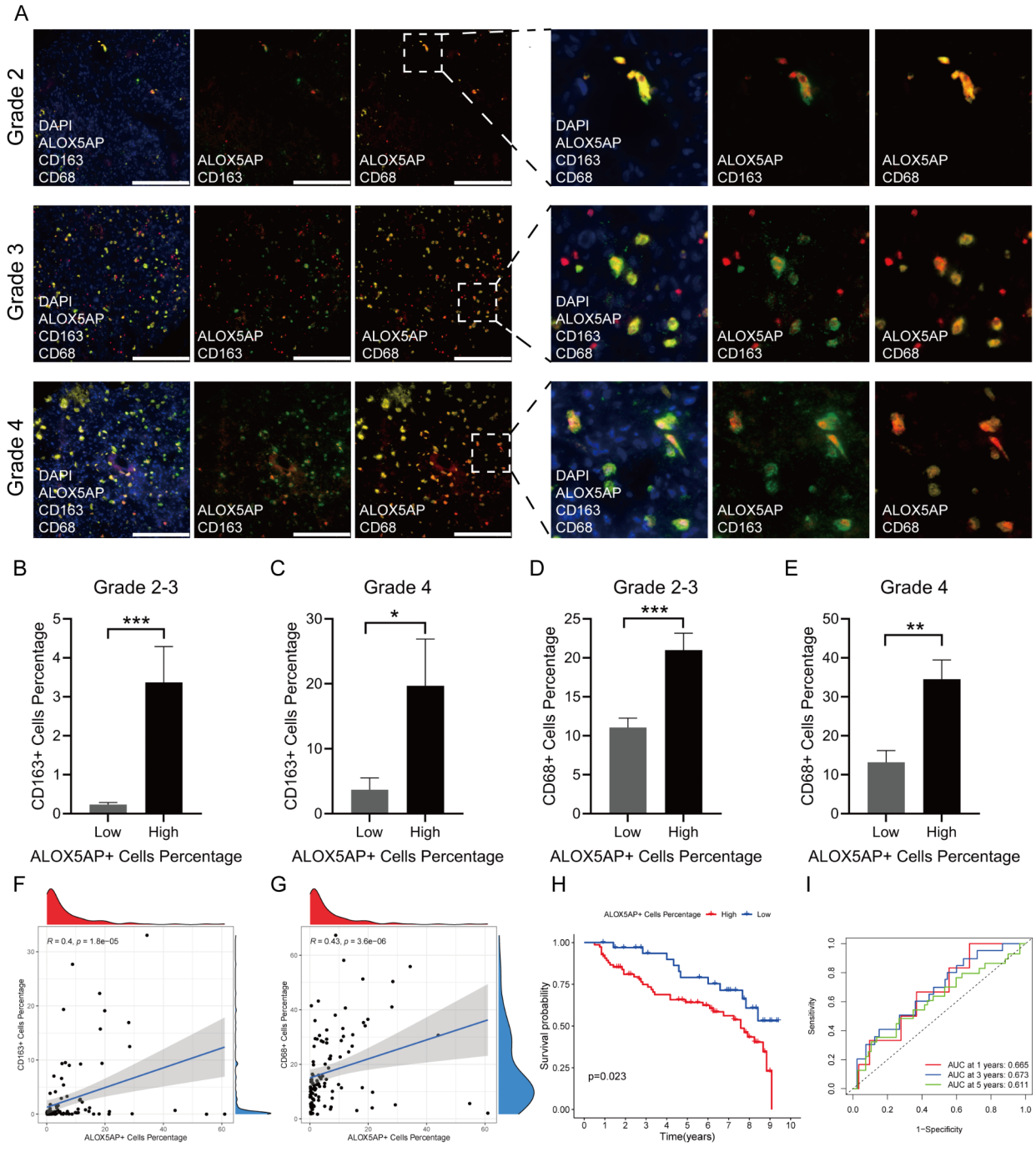

Fig. 10 Validation of ALOX5AP in relationship to macrophage markers and prognosis in glioma tissue microarray. **A** The colocalization of ALOX5AP (red), CD163 (green), and CD68 (yellow) in glioma (The scale bar is 200 μm). **B**, **C** Difference analysis of CD163 + cell percentage in high and low ALOX5AP + cell percentage group. **D**, **E** Difference analysis of CD68 + cell percentage in high and low ALOX5AP + cell percentage group. **F**, **G** The correlation between the ALOX5AP + cells percentage and the CD163 + cells percentage and CD68 + cell percentage. **H** Kaplan-Meier curve; **I** time-ROC curve. *$P < 0.05$, **$P < 0.01$, ***$P < 0.001$

accurately predicted glioma OS at 1 (AUC=0.665), 3 (AUC=0.637), and 5years (AUC=0.611) (Fig. 10I).

Discussion

AA metabolic pathways are important in inflammation and inflammation-associated carcinogenesis. Inhibition of the 5-lipoxygenase pathways clearly has preventive effects on various cancers [37]. ALOX5AP is an integral protein in the LOX metabolic pathway of AA. However, the evidence for the effect of ALOX5AP on glioma is very preliminary and lacks experimental validation. The small molecule inhibitor of ALOX5AP, MK886, is known to show anti-tumor activity in a variety of human cell lines, and this inhibition may be related to actin B and the adhesion components [38]. In glioma cell lines, MK886 has also been reported to inhibit the growth of glioma cell lines U87MG and A172 [39]. Our research revealed that ALOX5AP is highly expressed in gliomas, particularly in GBM. ALOX5AP was observed to be upregulated in gliomas with malignant phenotypes, including WHO grade 2–3 and 4, IDH wild-type, 1p19q non-codeletion, and MGMTp unmethylated status. Notably, IDH mutation status and MGMTp methylation status were identified as significant prognostic biomarkers in glioma [40]. IDH-mutant gliomas typically manifest as lower-grade gliomas with a median OS exceeding 12 years. IDH-mutant gliomas with 1p19q codeletion, termed oligodendroglioma, exhibit the best prognosis whereas IDH wild-type gliomas usually present as GBM, with a median OS of 12–15 months [41]. These results suggest that ALOX5AP expression is upregulated in gliomas and may be associated with tumor progression.

The findings of our study indicate that ALOX5AP can be utilized as an independent prognostic factor for glioma, irrespective of age, sex, WHO grade, IDH mutation, 1p19q codeletion, and MGMTp methylation status. The nomogram constructed using the aforementioned characteristics also showed good predictive performance. The AUC of time-ROC curve displayed a reliable result, confirming ALOX5AP as a good predictor of 1-, 3-, 5-, and 10- year survival in patients with glioma. The bioinformatics results were validated using glioma tissue microarray data. Chen et al. have reported that ALOX5AP is upregulated in acute myeloid leukemia and is associated with a poor prognosis [42]. Ye et al. investigated the prognostic value and function of ALOX5AP and found that ALOX5AP was upregulated in serous ovarian cancer and utilized as a prognostic predictor for serous ovarian cancer patients [15]. Mining the TCGA database, Xu et al. found that ALOX5AP was considered to be correlated with poor overall survival in ovarian cancer [43]. Liu et al. construct a prognostic model of the nine key genes (ALOX5AP, ARHGAP15, CCL8, FCER1G, GBP4, HCK, MMP9, RARRES2, and TRIM22) in metastatic melanoma [44] Guan et al. employed bioinformatics analysis to identify ALOX5AP, HLA-DMB, HLA-DRA, and SPINT2 as prognostic markers of osteosarcoma metastasis [14]. In glioma, a model was established based on stemness index-based signature including seven genes (ADAP2, ALOX5AP, APOBEC3C, FCGRT, GNG5, LRRC25, and SP100) for risk stratification and survival prediction of LGG [16]. Ji et al. proposed a leukotriene synthesis-related M2 macrophage gene signature including PIK3R5, PIK3R6, ALOX5, ALOX5AP, and ALOX15B, which was associated with T-cell dysfunction and predicted an unfavorable outcome of glioma [45]. These findings suggest that ALOX5AP is a promising prognostic marker in a wide range of cancer types and deserves further investigation.

Our findings also revealed that ALOX5AP is predominantly expressed in macrophages, monocytes, and T cells, with minimal tumor cell expression. The ALOX5AP high expression group exhibited high M2 macrophage and neutrophil content, indicating that ALOX5AP expression positively correlated with immunosuppressive cell infiltration and negatively correlated with immune-activated cells. This suggests that ALOX5AP expression contributes to shaping the immunosuppressed immune microenvironment. Moreover, ALOX5AP co-localized with M2 macrophage markers by immunofluorescence staining, suggesting that ALOX5AP may be associated with M2 polarization in macrophages. M2 macrophages have been demonstrated to exert a range of pro-tumorigenic activities including promoting tumor proliferation, invasion, angiogenesis, and an immunosuppressive TME [46]. ALOX5AP has previously been identified as a characteristic gene of M2 macrophages [45]. Consequently, ALOX5AP may exert pro-tumor effects by reprogramming macrophage phenotypes.

The evaluation of GBM using the TISIDB database highlighted known tumor immunosuppressive factors including CSF1R, HAVCR2, and IL-10. CSF1R is a key factor in macrophage recruitment and immunosuppressive polarization, with its inhibition altering macrophage polarization and reversing the immunosuppressive TME by supporting anti-tumor T-cell responses [47, 48]. TIM-3, also known as HAVCR2, is an activation-induced inhibitory molecule that induces T-cell exhaustion [49]. Additionally, TIM-3 is present on the surface of macrophages and facilitates their M2 polarization through its interaction with Gal9, which is derived from PTEN-deficient GBM cells [50]. IL-10 mediates the glioma immunosuppressive TME and is associated with T cell dysfunction [51, 52]. Our study also revealed that ALOX5AP is associated with several chemokines (i.e., CCL2, CCL20, CCL20, CXCL8, and CXCL16) and chemokine receptors (i.e., CCR1, CCR2, and CCR5). CCL2–CCR2, CXCL8–CCR2, and CXCL6–CXCR6 signaling

drives TAMs toward an anti-inflammatory phenotype and fosters tumor growth and invasion [53–55]. Thus, ALOX5AP is associated with T-cell exhaustion-associated cytokines and signaling pathways, suggesting that it may contribute to immune evasion in gliomas.

Traditionally, tumors with higher TMB levels were considered more immunogenic, easily recognized by the immune system, and likely to benefit from immunotherapy. Conversely, one study indicated that DNA mismatch repair deficiency-derived mutations are not sufficient to improve tumor immunogenicity and do not affect T-cell infiltration [56]. Compared with TMB or immune checkpoint used in isolation, the combination of TMB, HLA molecules, immune checkpoint, and other factors has better accuracy in predicting immunotherapy [36]. Thus, the elevated TMB and HLA molecules expression observed in the ALOX5AP high expression group did not definitively indicate the effectiveness of immunotherapy. The IPS is calculated by incorporating four key determinants of tumor immunogenicity, including effector cells, checkpoint/immunomodulator, antigen processing major histocompatibility complex molecules (such as HLA molecules), and immunosuppressive cells, with superior performance in predicting anti-PD-1 /CTLA-4 treatment of tumors [28]. The TIDE score mainly reflects two primary mechanisms of tumor immune evasion: T cell dysfunction and the prevention of T cell infiltration [29]. Our study showed that patients with high ALOX5AP expression had higher TIDE scores and IPS. Thus, the group with high ALOX5AP expression may be more prone to immune evasion, whereas targeting ALOX5AP may improve immunotherapeutic efficacy. Consistent with this, patients with high ALOX5AP expression exhibited reduced showed lower sensitivity to TMZ, a first-line glioma chemotherapy drug. Additionally, M2 TAMs are also thought to be associated with T cell exhaustion and chemotherapy resistance [8, 57]. Macrophage-derived ALOX5AP may contribute to these characteristics and may serve as a potential marker for immunotherapeutic response and chemotherapeutics drugs sensitivity.

Furthermore, GSEA results showed that ALOX5AP was enriched in chemokine signaling pathways and cytokine–cytokine receptors, highlighting the potential immunoregulatory role of ALOX5AP through its involvement in the aforementioned pathways. Cytokines mediate cell communication within the immune microenvironment and have complex functions, including the promotion of tumor cell survival and proliferation (TGF-β, IL-1β, and CXCL12), immunosuppression (IL-10, IL-4, and TGF-β), and angiogenesis (TNF, IL-6, and various chemokines) [58]. Chemokines play a pivotal role in shaping the TME and regulating crucial processes such as angiogenesis, metastasis, stemness, and invasion [59]. The enrichment analysis of ALOX5AP PPI network indicated its involvement in fatty acid metabolism and biosynthesis, myeloid leukocyte, glial cell, and microglial cell activation, and inflammatory responses. These ALOX5AP-related pathways suggest that ALOX5AP is closely associated with the immune microenvironment.

Our study has some limitations. First, the transcriptome data utilized in this study were obtained exclusively from public databases. The reliability of the conclusions may be constrained by potential biases in database selection and variability in bioinformatics tools. Further experimental validation of these results with self-sequencing data is necessary in the future. Second, the limited number of WHO grade 4 gliomas in the glioma microarray may compromise the validation of prognosis and consequently impair the reliability of the results. Third, our study merely corroborated the co-localization and co-expression of ALOX5AP and macrophage markers through immunofluorescence. It is imperative to substantiate the expression levels of ALOX5AP in M0, M1, and M2 macrophages at the molecular and cellular levels through qPCR and Western blot. The function of ALOX5AP on tumor progression and therapeutic potential need to be validated in vivo and in vitro after the knockdown of ALOX5AP in macrophages.

Conclusions

Our study suggests that ALOX5AP may serve as a biomarker of glioma prognosis and immunotherapy response. ALOX5AP is expressed in M2 macrophages and is associated with various immune-related signaling pathways. These findings support further investigation of ALOX5AP as an potential target in glioma.

Abbreviations

5-HEPE	5-hydroperoxy eicosatetraenoic acid
AA	Arachidonic acid
ALOX5AP	Arachidonate 5-lipoxygenase activating protein
AUC	Area under the curve
BP	Biological process
CC	Cellular component
CGGA	Chinese Glioma Genome Atlas
GBM	Glioblastoma
GDSC	Genomics of Drug Sensitivity in Cancer
GEPIA	Gene Expression Profiling Interaction Analysis
GO	Gene ontology
GSEA	Gene Set Enrichment Analysis
IDH	Isocitrate dehydrogenase
IPS	Immunophenoscore
KEGG	Kyoto Encyclopedia of Genes and Genomes database
LGG	Lower-grade glioma
LOX	Lipoxygenase
MF	Molecular function
MGMTp	O^6-methylguanine-DNA methyltransferase promoter
OS	Overall survival
RNA-Seq	RNA-sequencing
TAM	Tumour-associated macrophage
TCGA	The Cancer Genome Atlas
TCIA	The Cancer Immunome Atlas
TIDE	Tumor Immune Dysfunction and Exclusion
TIMER	Tumor Immune Estimation Resource
Time-ROC	Time-dependent receiver operating characteristic

TISCH2	The Tumor Immune Single Cell Hub 2
TMB	Tumour mutation burden
TME	Tumour microenvironment
TMZ	Temozolomide
WHO	World Health Organization

Supplementary Information

The online version contains supplementary material available at https://doi.org/10.1186/s12920-024-01991-8.

Supplementary Material 1

Supplementary Material 2

Supplementary Material 3

Supplementary Material 4

Acknowledgements
Not applicable.

Author contributions
Ping Song：Writing-original draft, Methodology, Data Curation, Formal analysis, Investigation. Hui Deng: Writing-review and editing, Methodology, Validation. Yushu Liu: Investigation, Validation. Mengxian Zhang: Conceptualization, Resources, Supervision, Writing-review and editing.

Funding
This study was supported by the National Natural Science Foundation of China (No.81772680).

Data availability
No datasets were generated or analysed during the current study.

Declarations

Ethics approval and consent to participate
Ethical approval for the study of the tissue microarray slide was granted by the Sample bank Ethics Committee of Shanghai Outdo Biotech Company (Shanghai, China) and all the participants provided written informed consent.

Consent for publication
Not applicable.

Competing interests
The authors declare no competing interests.

Author details
[1]Department of Oncology, Tongji Hospital, Tongji Medical College, Huazhong University of Science and Technology, Hubei, Wuhan 430030, P.R. China

Received: 19 April 2024 / Accepted: 13 August 2024
Published online: 21 August 2024

References

1. Schaff LR, Mellinghoff IK. Glioblastoma and other primary brain malignancies in adults: a review. JAMA. 2023;329:574–87.
2. Ostrom QT, Cioffi G, Gittleman H, Patil N, Waite K, Kruchko C, et al. CBTRUS Statistical Report: primary brain and other Central Nervous System tumors diagnosed in the United States in 2012–2016. Neuro Oncol. 2019;21:v1–100.
3. Wen PY, Weller M, Lee EQ, Alexander BM, Barnholtz-Sloan JS, Barthel FP, et al. Glioblastoma in adults: a Society for Neuro-Oncology (SNO) and European Society of Neuro-Oncology (EANO) consensus review on current management and future directions. Neuro Oncol. 2020;22:1073–113.
4. Quail DF, Joyce JA. The Microenvironmental Landscape of Brain tumors. Cancer Cell. 2017;31:326–41.
5. Charles NA, Holland EC, Gilbertson R, Glass R, Kettenmann H. The brain tumor microenvironment. Glia. 2011;59:1169–80.
6. Chen Z, Feng X, Herting CJ, Garcia VA, Nie K, Pong WW, et al. Cellular and Molecular Identity of Tumor-Associated macrophages in Glioblastoma. Cancer Res. 2017;77:2266–78.
7. Sica A, Mantovani A. Macrophage plasticity and polarization: in vivo veritas. J Clin Invest. 2012;122:787–95.
8. Chen Q, Jin J, Huang X, Wu F, Huang H, Zhan R. EMP3 mediates glioblastoma-associated macrophage infiltration to drive T cell exclusion. J Exp Clin Cancer Res. 2021;40:160.
9. Lee AH, Sun L, Mochizuki AY, Reynoso JG, Orpilla J, Chow F, et al. Neoadjuvant PD-1 blockade induces T cell and cDC1 activation but fails to overcome the immunosuppressive tumor associated macrophages in recurrent glioblastoma. Nat Commun. 2021;12:6938.
10. Gomes RN, Felipe da Costa S, Colquhoun A. Eicosanoids and cancer. Clinics.2018;73.
11. Gerstmeier J, Weinigel C, Rummler S, Radmark O, Werz O, Garscha U. Time-resolved in situ assembly of the leukotriene-synthetic 5-lipoxygenase/5-lipoxygenase-activating protein complex in blood leukocytes. FASEB J. 2016;30:276–85.
12. Zhang Y, Yang J, Zhang J, Sun L, Hirankarn N, Pan HF, et al. Genome-wide search followed by replication reveals genetic interaction of CD80 and ALOX5AP associated with systemic lupus erythematosus in Asian populations. Ann Rheum Dis. 2016;75:891–8.
13. Mashima R, Okuyama T. The role of lipoxygenases in pathophysiology; new insights and future perspectives. Redox Biol. 2015;6:297–310.
14. Guan X, Guan Z, Song C. Expression profile analysis identifies key genes as prognostic markers for metastasis of osteosarcoma. Cancer Cell Int. 2020;20:104.
15. Ye X, An L, Wang X, Zhang C, Huang W, Sun C, et al. ALOX5AP predicts poor prognosis by enhancing M2 macrophages polarization and immunosuppression in Serous Ovarian Cancer Microenvironment. Front Oncol. 2021;11:675104.
16. Zhang M, Wang X, Chen X, Guo F, Hong J. Prognostic value of a Stemness Index-Associated signature in primary Lower-Grade Glioma. Front Genet. 2020;11:441.
17. Lee H, Palm J, Grimes SM, Ji HP. The Cancer Genome Atlas Clinical Explorer: a web and mobile interface for identifying clinical-genomic driver associations. Genome Med. 2015;7:112.
18. Zhao Z, Zhang KN, Wang Q, Li G, Zeng F, Zhang Y, et al. Chinese Glioma Genome Atlas (CGGA): a Comprehensive Resource with functional genomic data from Chinese glioma patients. Genomics Proteom Bioinf. 2021;19:1–12.
19. Barrett T, Wilhite SE, Ledoux P, Evangelista C, Kim IF, Tomashevsky M, et al. NCBI GEO: archive for functional genomics data sets–update. Nucleic Acids Res. 2013;41:D991–5.
20. Li B, Severson E, Pignon JC, Zhao H, Li T, Novak J, et al. Comprehensive analyses of tumor immunity: implications for cancer immunotherapy. Genome Biol. 2016;17:174.
21. Tang Z, Li C, Kang B, Gao G, Li C, Zhang Z. GEPIA: a web server for cancer and normal gene expression profiling and interactive analyses. Nucleic Acids Res. 2017;45:W98–102.
22. Ianevski A, Giri AK, Aittokallio T. Fully-automated and ultra-fast cell-type identification using specific marker combinations from single-cell transcriptomic data. Nat Commun. 2022;13:1246.
23. Armstrong G, Martino C, Rahman G, Gonzalez A, Vázquez-Baeza Y, Mishne G, et al. Uniform Manifold Approximation and Projection (UMAP) reveals composite patterns and resolves visualization artifacts in Microbiome Data. Volume 6. mSystems; 2021. p. e0069121.
24. Sun D, Wang J, Han Y, Dong X, Ge J, Zheng R, et al. TISCH: a comprehensive web resource enabling interactive single-cell transcriptome visualization of tumor microenvironment. Nucleic Acids Res. 2021;49:D1420–30.
25. Yoshihara K, Shahmoradgoli M, Martínez E, Vegesna R, Kim H, Torres-Garcia W, et al. Inferring tumour purity and stromal and immune cell admixture from expression data. Nat Commun. 2013;4:2612.
26. Newman AM, Liu CL, Green MR, Gentles AJ, Feng W, Xu Y, et al. Robust enumeration of cell subsets from tissue expression profiles. Nat Methods. 2015;12:453–7.
27. Ru B, Wong CN, Tong Y, Zhong JY, Zhong SSW, Wu WC, et al. TISIDB: an integrated repository portal for tumor-immune system interactions. Bioinformatics. 2019;35:4200–2.
28. Charoentong P, Finotello F, Angelova M, Mayer C, Efremova M, Rieder D, et al. Pan-cancer immunogenomic analyses reveal genotype-immunophenotype

relationships and predictors of response to checkpoint blockade. Cell Rep. 2017;18:248–62.
29. Jiang P, Gu S, Pan D, Fu J, Sahu A, Hu X, et al. Signatures of T cell dysfunction and exclusion predict cancer immunotherapy response. Nat Med. 2018;24:1550–8.
30. Yang W, Soares J, Greninger P, Edelman EJ, Lightfoot H, Forbes S, et al. Genomics of Drug Sensitivity in Cancer (GDSC): a resource for therapeutic biomarker discovery in cancer cells. Nucleic Acids Res. 2013;41:D955–61.
31. Reimand J, Isserlin R, Voisin V, Kucera M, Tannus-Lopes C, Rostamianfar A, et al. Pathway enrichment analysis and visualization of omics data using g:Profiler, GSEA, Cytoscape and EnrichmentMap. Nat Protoc. 2019;14:482–517.
32. Szklarczyk D, Gable AL, Lyon D, Junge A, Wyder S, Huerta-Cepas J, et al. STRING v11: protein-protein association networks with increased coverage, supporting functional discovery in genome-wide experimental datasets. Nucleic Acids Res. 2019;47:D607–13.
33. Shannon P, Markiel A, Ozier O, Baliga NS, Wang JT, Ramage D, et al. Cytoscape: a software environment for integrated models of biomolecular interaction networks. Genome Res. 2003;13:2498–504.
34. Wang LC, Wang YL, He B, Zheng YJ, Yu HC, Liu ZY, et al. Expression and clinical significance of VISTA, B7-H3, and PD-L1 in glioma. Clin Immunol. 2022;245:109178.
35. Yarchoan M, Hopkins A, Jaffee EM. Tumor mutational burden and response rate to PD-1 inhibition. N Engl J Med. 2017;377:2500–1.
36. Jardim DL, Goodman A, de Melo Gagliato D, Kurzrock R. The challenges of Tumor Mutational Burden as an Immunotherapy Biomarker. Cancer Cell. 2021;39:154–73.
37. Chen X, Sood S, Yang CS, Li N, Sun Z. Five-lipoxygenase pathway of arachidonic acid metabolism in carcino-genesis and cancer chemoprevention. Curr Cancer Drug Targets. 2006;6:613–22.
38. Mayburd AL, Martlinez A, Sackett D, Liu H, Shih J, Tauler J, et al. Ingenuity network-assisted transcription profiling: identification of a new pharmacologic mechanism for MK886. Clin Cancer Res. 2006;12:1820–7.
39. Lim JY, Oh JH, Jung JR, Kim SM, Ryu CH, Kim HT, et al. MK886-induced apoptosis depends on the 5-LO expression level in human malignant glioma cells. J Neurooncol. 2010;97:339–46.
40. Yang K, Wu Z, Zhang H, Zhang N, Wu W, Wang Z, et al. Glioma targeted therapy: insight into future of molecular approaches. Mol Cancer. 2022;21:39.
41. Nicholson JG, Fine HA. Diffuse glioma heterogeneity and its therapeutic implications. Cancer Discov. 2021;11:575–90.
42. Chen XY, Wen XM, Zhao W, Chu MQ, Gu Y, Huang HH, et al. ALOX5AP is a new prognostic indicator in acute myeloid leukemia. Discov Oncol. 2023;14:210.
43. Xu Y, Xu Y, Wang C, Xia B, Mu Q, Luan S, et al. Mining TCGA database for gene expression in ovarian serous cystadenocarcinoma microenvironment. PeerJ. 2021;9:e11375.
44. Liu J, Zhang X, Ye T, Dong Y, Zhang W, Wu F, et al. Prognostic modeling of patients with metastatic melanoma based on tumor immune microenvironment characteristics. Math Biosci Eng. 2022;19:1448–70.
45. Ji H, Liu Z, Wang N, Jin J, Zhang J, Dong J, et al. Integrated genomic, transcriptomic, and epigenetic analyses identify a leukotriene synthesis-related M2 macrophage gene signature that predicts prognosis and treatment vulnerability in gliomas. Front Immunol. 2022;13:970702.
46. Wang G, Zhong K, Wang Z, Zhang Z, Tang X, Tong A, et al. Tumor-associated microglia and macrophages in glioblastoma: from basic insights to therapeutic opportunities. Front Immunol. 2022;13:964898.
47. Fermi V, Warta R, Wöllner A, Lotsch C, Jassowicz L, Rapp C et al. Effective reprogramming of patient-derived M2-polarized glioblastoma-associated microglia/macrophages by treatment with GW2580. Clin Cancer Res.2023.
48. Pyonteck SM, Akkari L, Schuhmacher AJ, Bowman RL, Sevenich L, Quail DF, et al. CSF-1R inhibition alters macrophage polarization and blocks glioma progression. Nat Med. 2013;19:1264–72.
49. Huang Y-H, Zhu C, Kondo Y, Anderson AC, Gandhi A, Russell A, et al. CEACAM1 regulates TIM-3-mediated tolerance and exhaustion. Nature. 2014;517:386–90.
50. Ni X, Wu W, Sun X, Ma J, Yu Z, He X, et al. Interrogating glioma-M2 macrophage interactions identifies Gal-9/Tim-3 as a viable target against PTEN-null glioblastoma. Sci Adv. 2022;8:eabl5165.
51. Widodo SS, Dinevska M, Furst LM, Stylli SS, Mantamadiotis T. IL-10 in glioma. Br J Cancer. 2021;125:1466–76.
52. Ravi VM, Neidert N, Will P, Joseph K, Maier JP, Kückelhaus J, et al. T-cell dysfunction in the glioblastoma microenvironment is mediated by myeloid cells releasing interleukin-10. Nat Commun. 2022;13:925.
53. Lepore F, D'Alessandro G, Antonangeli F, Santoro A, Esposito V, Limatola C et al. CXCL16/CXCR6 Axis Drives Microglia/Macrophages Phenotype in physiological conditions and plays a crucial role in Glioma. Frontiers in Immunology.2018;9.
54. Flores-Toro JA, Luo D, Gopinath A, Sarkisian MR, Campbell JJ, Charo IF, et al. CCR2 inhibition reduces tumor myeloid cells and unmasks a checkpoint inhibitor effect to slow progression of resistant murine gliomas. Proc Natl Acad Sci U S A. 2020;117:1129–38.
55. Yuan W, Zhang Q, Gu D, Lu C, Dixit D, Gimple RC et al. Dual role of CXCL8 in maintaining the mesenchymal state of glioblastoma stem cells and M2-like tumor-associated macrophages. Clin Cancer Res.2023.
56. Westcott PMK, Muyas F, Hauck H, Smith OC, Sacks NJ, Ely ZA, et al. Mismatch repair deficiency is not sufficient to elicit tumor immunogenicity. Nat Genet. 2023;55:1686–95.
57. Zhang G, Tao X, Ji B, Gong J. Hypoxia-driven M2-Polarized macrophages facilitate Cancer Aggressiveness and Temozolomide Resistance in Glioblastoma. Oxid Med Cell Longev. 2022;2022:1614336.
58. Propper DJ, Balkwill FR. Harnessing cytokines and chemokines for cancer therapy. Nat Rev Clin Oncol. 2022;19:237–53.
59. Bule P, Aguiar SI, Aires-Da-Silva F, Dias JNR. Chemokine-Directed Tumor Microenvironment Modulation in Cancer Immunotherapy. Int J Mol Sci.2021;22.

Publisher's Note